The Journal of Infectious Diseases

MAJOR ARTICLE

Membrane Lipids Augment Cell Envelope Stress Signaling via the MadRS System to Defend Against Antimicrobial Peptides and Antibiotics in *Enterococcus faecalis*

William R. Miller,[1,2,3] April Nguyen,[1,2,4,5] Kavindra V. Singh,[1,2] Samie Rizvi,[1,2] Ayesha Khan,[4,5,a] Sam G. Erickson,[4] Stephanie L. Egge,[1,2] Melissa Cruz,[4,5] An Q. Dinh,[1,2] Lorena Diaz,[6,7] Philip C. Thornton,[1,2] Rutan Zhang,[8] Libin Xu,[8] Danielle A. Garsin,[4,5] Yousif Shamoo,[9] and Cesar A. Arias[1,2,3]

[1]Division of Infectious Diseases, Houston Methodist Hospital, Houston, Texas, USA; [2]Center for Infectious Diseases, Houston Methodist Research Institute, Houston, Texas, USA; [3]Department of Medicine, Weill Cornell Medical College, New York, New York, USA; [4]McGovern Medical School, University of Texas Health Science Center, Houston, Texas, USA; [5]Microbiology and Molecular Genetics, Graduate School of Biomedical Sciences, University of Texas Health Science Center, Houston, Texas, USA; [6]Genomics and Resistant Microbes Group, Facultad de Medicina Clinica Alemana, Universidad del Desarrollo, Santiago, Chile; [7]Molecular Genetics and Antimicrobial Resistance Unit, Universidad El Bosque, Bogota, Colombia; [8]Department of Medicinal Chemistry, University of Washington, Seattle, Washington, USA; and [9]Department of Biosciences, Rice University, Houston, Texas, USA

(See the Editorial Commentary by Supandy and Van Tyne on pages 287–90.)

Enterococci have evolved resistance mechanisms to protect their cell envelopes against bacteriocins and host cationic antimicrobial peptides (CAMPs) produced in the gastrointestinal environment. Activation of the membrane stress response has also been tied to resistance to the lipopeptide antibiotic daptomycin. However, the actual effectors mediating resistance have not been elucidated. Here, we show that the MadRS (formerly YxdJK) membrane antimicrobial peptide defense system controls a network of genes, including a previously uncharacterized 3-gene operon (*madEFG*) that protects the *Enterococcus faecalis* cell envelope from antimicrobial peptides. Constitutive activation of the system confers protection against CAMPs and daptomycin in the absence of a functional LiaFSR system and leads to persistence of cardiac microlesions in vivo. Moreover, changes in the lipid cell membrane environment alter CAMP susceptibility and expression of the MadRS system. Thus, we provide a framework supporting a multilayered envelope defense mechanism for resistance and survival coupled to virulence.

Keywords. *Enterococcus faecalis*; daptomycin; antimicrobial peptides; membrane lipids; cell envelope stress response.

Enterococci are a leading cause of health care-associated infections and possess a diverse array of antimicrobial resistance determinants [1, 2]. These organisms are colonizers of the gastrointestinal tract, where they are exposed to cationic antimicrobial peptides (CAMPs) produced by the innate immune system [3]. Several important antibiotics used in clinical practice, including the lipopeptide daptomycin, share functional similarities with CAMPs, and enterococci have evolved several mechanisms to sense and respond to these agents [4–8]. In particular, the LiaFSR system of *Enterococcus faecalis* has been linked to survival in the presence of daptomycin, the cathelicidin LL-37, and other CAMPs, via a secreted protein (LiaX), which plays a dual sensing and regulatory role mediated by the N- and C-terminal domains, respectively [9]. Experimental evolution in the presence of daptomycin using both *E. faecalis* and *Enterococcus faecium* strains lacking the LiaR response regulator and deficient in LiaFSR signaling suggested that activation of the YxdJK 2-component system in the presence of mutations in *dak* (encoding a putative fatty acid kinase) could also lead to the development of daptomycin resistance [5, 10].

The YxdJK system shares homology with other ABC transporters involved in lantibiotic and antimicrobial peptide resistance, including the BceRS-BceAB system from *Bacillus subtilis* and the GraRS-VraDE system from *Staphylococcus aureus* [11]. YxdJK and its downstream effectors function as a transcriptional unit; however, these genes are located in multiple locations throughout the enterococcal chromosome. Dak is a homologue of the fatty acid kinase Fak in *S. aureus*, responsible for the first step in incorporation of exogenous fatty acids into bacterial phospholipids [12]. Fatty acids have been implicated in increasing survival in the presence of daptomycin and other membrane stressors [13]. As the specific mechanism by which *E. faecalis* defends the cell envelope against CAMPs is unknown, we sought to determine the role of *dak* and the YxdJK system (which we hereafter refer to as the MadRS system for membrane antimicrobial peptide defense), in cell envelope protection against daptomycin and host-derived CAMPs.

Received 03 November 2023; editorial decision 14 February 2024; accepted 03 April 2024; published online 5 April 2024

[a]Current affiliation: Department of Pathology, Microbiology, and Immunology, Vanderbilt University Medical Center, Nashville, TN.

Presented in part: IDWeek October 2021, Virtual Meeting; and the American Society for Microbiology Microbe conference June 2023, Houston, Texas, USA.

Correspondence: William Miller, MD, Division of Infectious Diseases, Houston Methodist Hospital, 6560 Fannin Street, Scurlock Tower Suite 1540, Houston 77030, TX (wrmiller@houstonmethodist.org).

The Journal of Infectious Diseases® 2025;231:307–17

https://doi.org/10.1093/infdis/jiae173

METHODS

Genetic Manipulation of Strains

For details, please refer to the Supplementary Methods. Bacterial strains and plasmids used in this work are listed in Supplementary Table 1; primers are listed in Supplementary Table 2. Chromosomal deletions were generated using the pCE plasmid and a derivative of OG1RF with the *E. faecalis* ATCC 4200 CRISPR1 *cas9* gene inserted in a neutral genomic insertion site to aid in genetic manipulation, as previously described [14, 15].

RNA Sequence Analysis and qRT-PCR

RNA sequence analysis and quantitative reverse-transcription polymerase chain reaction (qRT-PCR) were performed as previously described [9]. Strains were grown overnight in tryptic soy broth (TSB; Becton Dickinson) plus 50 mg/L of calcium chloride, then diluted into fresh TSB with Ca^{2+} alone or with daptomycin or bacitracin-zinc at 50% of the minimum inhibitory concentration (MIC). RNA was isolated after growth to mid-exponential phase at 37°C. Sequencing was performed on an Illumina HiSeq2000. Reads were mapped using the OG1RF genome. qRT-PCR was performed using SYBR Green in a CFX96 Touch Real-Time PCR Detection System (Bio-Rad; primers are listed in Supplementary Table 2). For all experiments, expression level was quantified relative to the control strain, OG1RF, without antibiotic exposure.

Antimicrobial Peptide Killing Assays

Antimicrobial peptide killing assays for LL-37 (50 μg/mL; catalog No. AS-61302; Anaspec), HBD3 (6 μg/mL; catalog No. AS-60741; Anaspec), and HNP-1 (10 μg/mL; catalog No. AS-60743; Anaspec) were performed as previously described [16, 17]. Assay buffer of RPMI + 5% LB was used for LL-37 and HBD3, and 10 mM KH_2PO_4, pH 7.4 for HNP-1. Mid-exponential phase cultures were diluted in assay buffer to a final inoculum of 1×10^4 colony-forming units (CFU)/mL and incubated for 2 hours at 37°C with or without peptides. Cells were washed and dilutions plated for colony counts. Percent survival for each strain was calculated using the difference between treated strain and growth control.

Determination of Membrane Lipids by Hydrophilic Interaction Chromatography-Ion Mobility-Mass Spectrometry

Lipids were extracted by the method of Bligh and Dyer [18–20]. Lipids were separated on a Waters UPLC using a Phenomenex Kinetex hydrophilic interaction chromatography-ion (HILIC) column (2.1 × 100 mm, 1.7 μm) at a temperature of 40°C and a flow rate of 0.5 mL/minute [21, 22]. Lipid analysis was performed on a Waters Synapt G2-XS platform with calibration of ion mobility (IM) measurements [23]. Data analysis was performed using the Progenesis QI software (Nonlinear Dynamics) for alignment, peak detection, and normalization. Lipid identification was based on *m/z* (within 10 ppm mass accuracy), retention time, and collision cross-section with an in-house version of LipidPioneer and LiPydomics [22, 24, 25].

Caenorhabditis elegans Infection Model

A *C. elegans* infection model was used to assay virulence of OG1RF and derivatives in wild-type and *pmk-1* deficient nematodes [26, 27]. Synchronized young adult nematodes were infected and 60–90 nematodes were transferred to a liquid media of 80% MW9 buffer and 20% BHI broth in 96-well plates. Plates were incubated at 25°C and evaluated daily for nematode survival. Survival curves from 3 independent runs were plotted using Kaplan-Meier log rank analysis.

Mouse Peritonitis Infection Model

A previously established mouse peritonitis model was used for this study [28]. The protocol was approved by the University of Texas Health Science Center (UTHSC) Animal Welfare Committee (AWC-19-0058). Female 4 to 6-week-old outbred ICR mice (Envigo) weighing approximately 25 grams were inoculated via intraperitoneal injection and followed for 96 hours postinfection. At the time of death, spleen and heart were aseptically excised. Spleens were homogenized, diluted in saline, and plated onto BHI agar for colony counts. To assess for cardiac microlesions, hearts were placed in formalin at the time of removal then processed by the UTHSC pathology core laboratory [29]. Sections were imaged with a Keyence BZ-X700 microscope, the number of microlesions was determined for each section, and mean number of microlesions per section for each strain and the area of each lesion was determined using FIJI software [30].

RESULTS

Identification of the MadRS Regulon

We previously described an alanine to aspartate substitution at amino acid position 202 in the MadS histidine kinase associated with daptomycin resistance in *E. faecalis* [5]. In the OG1RF$madS_{A202E}$ strain, the MIC of daptomycin increased from 1.5 to 6 μg/mL and the MIC of bacitracin from 32 to 96 μg/mL (Table 1). In the OG117 background, introduction of the $madS_{A202E}$ allele combined with deletion of the *dak* gene led to an increase in daptomycin and bacitracin MICs. No strains exhibited changes in susceptibility or tolerance to killing with ampicillin or vancomycin, even with physiologic concentrations of bicarbonate (Supplementary Table 3). Because the MadRS system is known to mediate protection from bacitracin via the presence of the ABC transporter MadLM (YxdLM), we hypothesized that this transporter may also be involved in the daptomycin resistance phenotype, similar to VraDE in *S. aureus* [31, 32]. However, deletion of the genes encoding MadLM from the chromosome of the daptomycin-resistant *E. faecalis* OG117Δ*dak*$madS_{A202E}$ led to a decrease in the MIC of bacitracin, but not daptomycin (Table 1). Thus, we applied transcriptomics to identify additional genes that could impact daptomycin MIC.

Table 1. Antimicrobial Minimum Inhibitory Concentrations

Strain	DAP	BAC	AMP	VAN
OG1RF	1.5	32	0.5	2
OG1RFΔ*liaR*	0.047	4	0.5	2
OG1RFΔ*madR*	0.38	12	0.5	3
OG1RF*madS*$_{A202E}$	6	96	1	3
OG117	1.5	32	0.75	3
OG117Δ*dak*	0.75	16	0.75	1.5
OG117Δ*dak::dak*	1.5	32	0.75	3
OG117Δ*dakmadS*$_{A202E}$	12	64	0.75	3
OG117Δ*dakmadS*$_{A202E}$Δ*madLM*	12	8	0.75	3
OG117Δ*dakmadS*$_{A202E}$Δ*madEFG*	12	64	0.75	3
OG117Δ*dakmadS*$_{A202E}$Δ*madEFG::madEFG*	8	64	1.5	3
OG117Δ*dakmadS*$_{A202E}$Δ*madEFG*Δ*madLM*	8	8	0.75	3
OG117Δ*dakmadS*$_{A202E}$Δ*dltA*	1.5	32	0.75	2
OG117Δ*dakmadS*$_{A202E}$Δ*dltA::dltA*	12	64	0.75	3
OG117Δ*liaX*	12	24	1	3
OG117Δ*liaX*Δ*madEFG*	12	24	1	3
OG117Δ*liaX*Δ*madEFG::madEFG*	16	24	0.75	3
OG117Δ*liaX*Δ*dltA*	2	32	1	2
OG117Δ*liaX*Δ*dltA::dltA*	12	24	0.75	3

All values μg/mL.

Abbreviations: AMP, ampicillin; BAC, bacitracin; DAP, daptomycin; VAN, vancomycin.

We compared differentially expressed genes in OG1RFΔ*madR*, which lacks the response regulator of the MadRS system, and OG1RF*madS*$_{A202E}$ to the parent strain OG1RF in the presence and absence of daptomycin (Figure 1*A* and 1*B*, and Supplementary Table 2). Comparing OG1RFΔ*madR* to OG1RF, there were 8 genes with a significant difference in expression without daptomycin exposure. The most strongly downregulated was a previously unidentified putative operon of 3 genes, *madEFG*, followed by *madLM*, as well as the genes *mprF2* (lysyl-PG-synthetase) and *salA* (peptidoglycan hydrolase). In OG1RF*madS*$_{A202E}$, there were 368 and 364 differentially expressed genes with and without daptomycin, respectively. These included increased expression of *madEFG*, the *dlt* operon, *madLM*, *salA*, and downregulation of *upp* (uracil phosphoribosyltransferase). We confirmed these results with qRT-PCR for the genes *madG*, *madL*, *dltA*, and *madA* (previously identified as part of the MadRS network). The *madR* knockout exhibited decreased gene expression of *madG* and *madL* compared to OG1RF, both with and without daptomycin. There was no significant difference in expression of either *madA* or *dltA*. The *madS*$_{A202E}$ background exhibited a significant increase in the expression of *madG*, *madL*, and *dltA*, particularly on daptomycin exposure (Figure 1*C*).

The MadRS Network Provides a Targeted Response to Antibiotics and Host-Derived AMPs

To study the effects of each component of the MadRS system, we constructed a series of deletion mutants targeting *madLM*, *madEFG*, and *dltA* in daptomycin-resistant OG117Δ*dakmadS*$_{A202E}$. Deletion of *madLM* or *madEFG* had no impact on the daptomycin MIC, while deletion of both led to a modest decrease (12 to 8 μg/mL). In contrast, deletion of *dltA* resulted in an 8-fold reduction in the daptomycin MIC. Because *madEFG* did not appear to alter susceptibility to bacitracin or daptomycin but were among the most significantly expressed genes under the control of MadR, we investigated alternative roles for MadEFG.

Given the similarities between daptomycin and CAMPs, we assayed the activity of several representative CAMPs, including LL-37 (cathelicidin), human β-defensin 3 (HBD3), and human neutrophil peptide-1 (HNP1, α-defensin) against the MadRS mutants (Figure 2*A* and 2*B*, and Supplementary Figure 1). In the presence of LL-37, OG117Δ*dakmadS*$_{A202E}$ exhibited a significant increase in survival versus OG117, and deletion of *madEFG*, but not *madLM* or *dltA*, resulted in increased killing by LL-37. Complementation with *madEFG* at the native chromosomal location restored bacterial survival. For HBD3, deletion of *dak* was sufficient to increase survival comparable to the OG117Δ*dakmadS*$_{A202E}$ mutant. Restoring the *dak* gene in the native chromosomal location restored HBD3 killing activity to wild-type levels. Loss of *madEFG* resulted in a decrease in HBD3 survival by 10.1%, but this was not statistically significant. No change in survival was seen for any strain with the α-defensin HNP1.

MadRS Mediates Survival in the Presence of CAMPs Independent of LiaFSR

We next sought to characterize the distinct roles of MadRS and LiaFSR in the cell envelope stress response. Exogenous N-terminal LiaX has been shown to activate LiaFSR signaling and provide protection against membrane stress even in daptomycin-sensitive *E. faecalis* isolates [9]. Introduction of the *madS*$_{A202E}$ allele into OG1RFΔ*liaR* (lacking activation of LiaFSR due to deletion of the gene encoding the response regulator) was sufficient to increase survival in the presence of LL-37 (Figure 2*C*), suggesting that a functional LiaFSR response was not necessary for MadRS-mediated protection. Conversely, deletion of the gene encoding the MadR response regulator in OG1RF resulted in decreased survival in the presence of LL-37, an effect that could not be rescued with the addition of exogenous LiaX, despite the strain retaining a functional LiaFSR system. A similar pattern was seen with daptomycin, with decreased survival in the *madR* deletion strain that could not be rescued by addition of LiaX (Figure 2*D*). These findings indicated that MadRS ultimately controls the effector systems responsible for CAMP resistance in *E. faecalis*.

To test this hypothesis, we made targeted deletions of the genes encoding MadEFG and DltA in the OG117Δ*liaX* background, where the LiaFSR system is constitutively expressed due to loss of the regulatory C-terminal domain of LiaX. Consistent with previous results, the OG117Δ*liaX* strain showed enhanced survival in the presence of LL-37 as compared to OG117 (Figure 2*E*). Deletion of *madEFG* in this

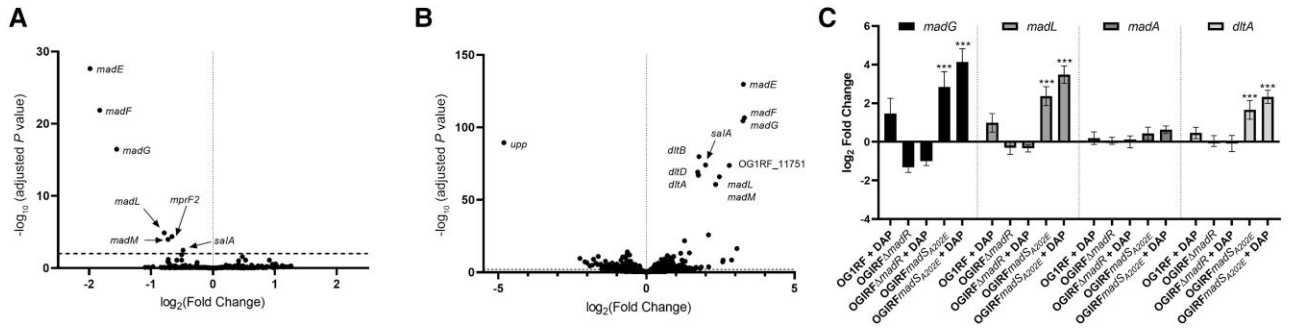

Figure 1. Transcriptional profile of the MadRS regulon. *A*, Gene expression by RNA sequence analysis of OG1RFΔ*madR* without daptomycin exposure as compared to wild-type OG1RF. The $\log_2$ fold change in gene expression is shown on the x-axis, and -$\log_{10}$ (adjusted *P* value) is shown on the y-axis. Horizontal dotted line represents the significance cutoff of $P < .01$. *B*, Differentially expressed genes in the OG1RF*madS*$_{A202E}$ as compared to OG1RF without daptomycin exposure. Select genes are labeled on the plot, a full list of differentially expressed genes can be found in Supplementary Table 4. *C*, qRT-PCR of representative genes of the MadRS system. Strains and antibiotic exposure conditions are shown on the x-axis. $\log_2$ fold change in gene expression is shown on the y-axis. Error bars represent the standard deviation of 3 independent biological runs performed in technical triplicate. Significant differences in gene expression were compared to OG1RF without exposure to daptomycin. ***$P < .001$. Abbreviations: DAP, daptomycin; qRT-PCR, quantitative reverse-transcription polymerase chain reaction.

background led to a decrease in survival, suggesting this system plays a significant role in membrane defense against LL-37, even in the presence of a constitutively active LiaFSR response. The loss of *dltA* led to decreased survival after exposure to LL-37 in the OG117Δ*liaX* background that was not statistically significant. Interestingly, in the OG117Δ*liaX* background loss of *madEFG* led to a significant decrease in survival in the presence of HBD3 (Figure 2*F*), suggesting that the MadRS system can respond to both β-defensins and cathelicidins.

MadEFG did not appear to directly impact daptomycin susceptibility; however, a reduction in the MIC of daptomycin from 12 to 2 μg/mL was observed in the OG117Δ*liaX*Δ*dltA* strain, and the MIC was restored on complementation of *dltA* in the native chromosomal location. Because D-alanylation of teichoic acids has been implicated in changes of cell surface charge and daptomycin resistance in *S. aureus*, we evaluated cell surface charge using a cytochrome c binding assay (Supplementary Figure 2). As compared to OG117, OG117Δ*liaX* displayed a significant increase in positive cell surface charge. This increase was abolished in the OG117Δ*liaX*Δ*dltA* strain and restored on complementation of *dltA*. In the OG117Δ*dak* background, there was an increase in cell surface charge of the *dak* deletion mutant, but no significant changes across the other strains. Thus, electrostatic repulsion cannot sufficiently explain the phenotypic changes observed in *E. faecalis*.

Loss of *dak* Alters the Membrane Lipid Environment and Leads to Activation of MadRS in the Absence of Antibiotic Stress

In the absence of *dak*, the endogenous type II fatty acid synthesis pathway (FASII) supplies acyl-chains for phospholipid synthesis. Consistent with this hypothesis, OG117Δ*dak* has increased sensitivity to triclosan (4 μg/mL), an inhibitor of the FabI enoyl-ACP reductase of FASII, as compared to wild-type OG117 or the *dak* complemented strain (both 16 μg/mL). During construction of the OG117Δ*dak* derivatives, we noted that OG117Δ*dakmadS*$_{A202E}$ and subsequent strains had a restoration of growth (Supplementary Figure 3). Whole-genome sequencing of these strains showed a serine to tyrosine change at amino acid 36 of FabT, a MarR transcriptional repressor, which binds upstream of the Fab operon (encoding the FASII enzymes). This change would be predicted to fall in the DNA binding domain, potentially impairing the binding of the repressor and resulting in constitutive expression of the Fab operon [33]. Colonies with the mutations in FabT had no change in triclosan susceptibility compared to OG117Δ*dak* (4 μg/mL), consistent with continued reliance on endogenous FA synthesis.

To assess membrane changes associated with the absence of *dak*, we performed hydrophilic interaction chromatography-mass spectrometry (HILIC-MS) to characterize the phospholipids of OG117, OG117Δ*dak*, the OG117Δ*dak*::*dak* complemented strain, and OG117Δ*dakmadS*$_{A202E}$ (Figure 3*A* and 3*B*) during exponential growth and stationary phase. In exponential phase, OG117Δ*dak* had a significant decrease in the abundance of phosphatidylglycerol (PG), lysyl-PG (LPG), and diacylglycerol (DG) as compared to OG117. In both the *dak* complemented and the OG117Δ*dakmadS*$_{A202E}$ strain (with the mutation in *fabT*), there were no significant changes in phospholipid abundance. In stationary phase, the OG117Δ*dakmadS*$_{A202E}$ strain had a significantly higher abundance of PG and LPG as compared to OG117, consistent with the increased expression of *mprF2* (the product of which synthesizes LPG) in the *madS*$_{A202E}$ mutant. The acyl chain composition of each lipid species in exponential and stationary phase is shown in Figure 3*C* and Supplementary Table 3. Strains with a deletion of *dak* showed a relative increase in shorter chain and saturated fatty acids as compared to OG117 during exponential phase growth.

To investigate whether the altered membrane environment associated with the deletion of *dak* influenced expression of the wild-type MadRS system, we evaluated the expression of *madG*

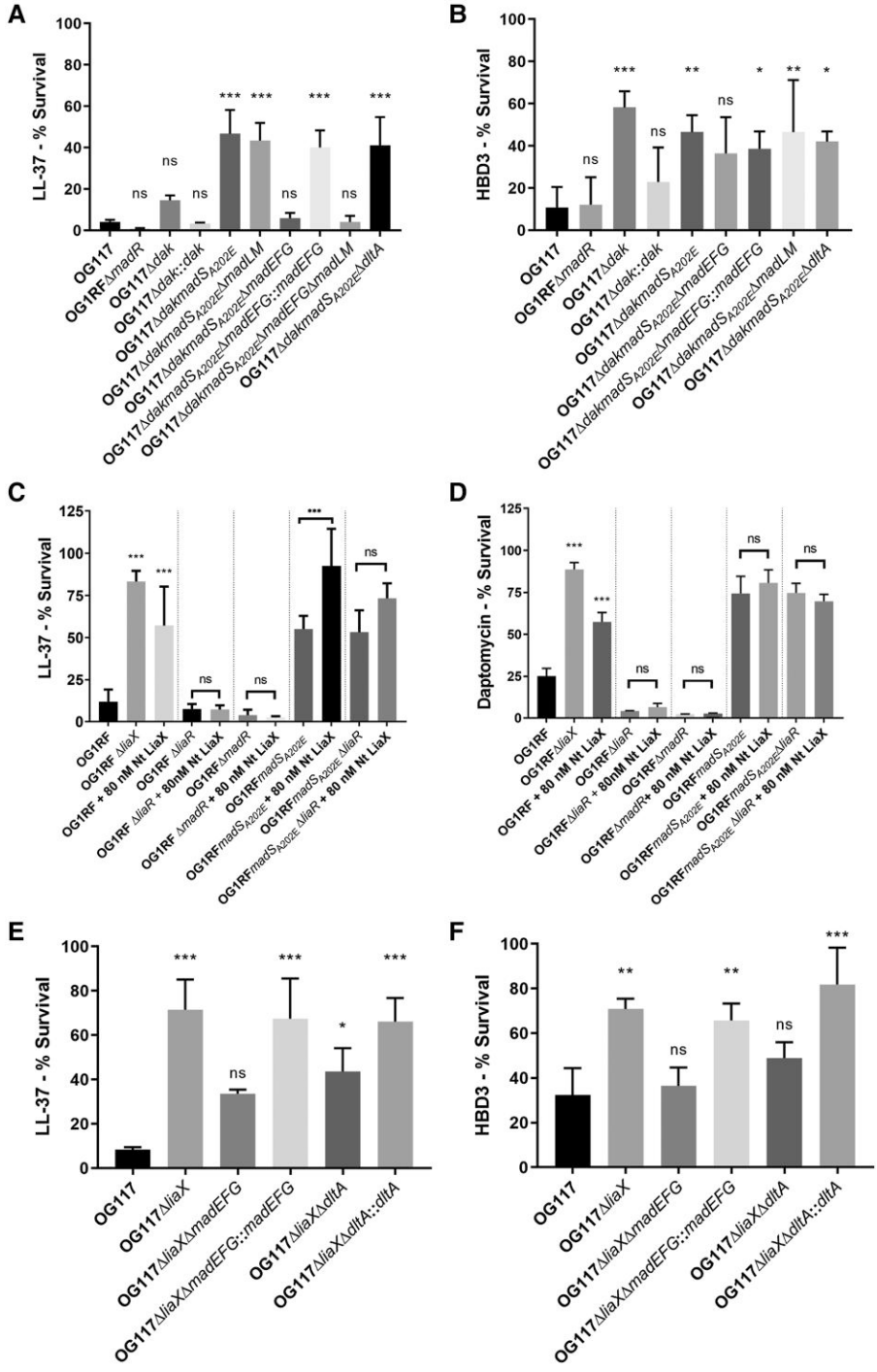

Figure 2. MadRS mediates survival in the presence of antimicrobial peptides and daptomycin independent of the LiaFSR system. *A*, LL-37 killing assay (50 µg/mL of LL-37) performed in OG117 background. Percent survival was calculated by dividing the colony forming units per milliliter (CFU/mL) of the peptide free growth control with the CFU/mL of the peptide-treated samples. The OG117Δ*dakmadS*$_{A202E}$ strain (daptomycin resistant) showed a significant increase in survival as compared to wild-type OG117. Deletion of *madEFG*, but not *madLM* alone or *dltA* led to increased killing by LL-37, and survival was restored on complementation of *madEFG* in the native chromosomal location. *B*, HBD3 killing assay (6 µg/mL of HBD3) performed in the OG117 background. Deletion of *dak* was sufficient to increase survival in the presence of HBD3. *C*, LL-37 and (*D*) daptomycin (4 µg/mL) killing assay in the OG1RF background, with and without the addition of N-terminal LiaX protein (Nt LiaX), previously shown to protect *Enterococcus faecalis* from LL-37–mediated killing in a LiaFSR-dependent manner. Nt LiaX was unable to rescue a MadR knockout strain (pairwise comparisons are shown as a bracket above strain pairs), and the presence of MadS$_{A202E}$ was able to confer increased survival in the presence of both LL-37 and daptomycin in a strain lacking a functional LiaFSR system (Δ*liaR*). *E*, LL-37 and (*F*) HBD3 killing assay in the OG117Δ*liaX* background with a constitutively active LiaFSR pathway. Deletion of *madEFG* decreased survival to a level that was not statistically different from wild type. In the absence of membrane changes induced by loss of *dak*, *madEFG* was also noted to be important for survival in the presence of HBD3. Significant differences in survival between each strain and OG117 were determined by 1-way ANOVA. Error bars represent the standard deviation of 3 independent runs, performed in biological triplicate on separate days. **P* < .05, ***P* < .01, ****P* < .001; ns, not significant.

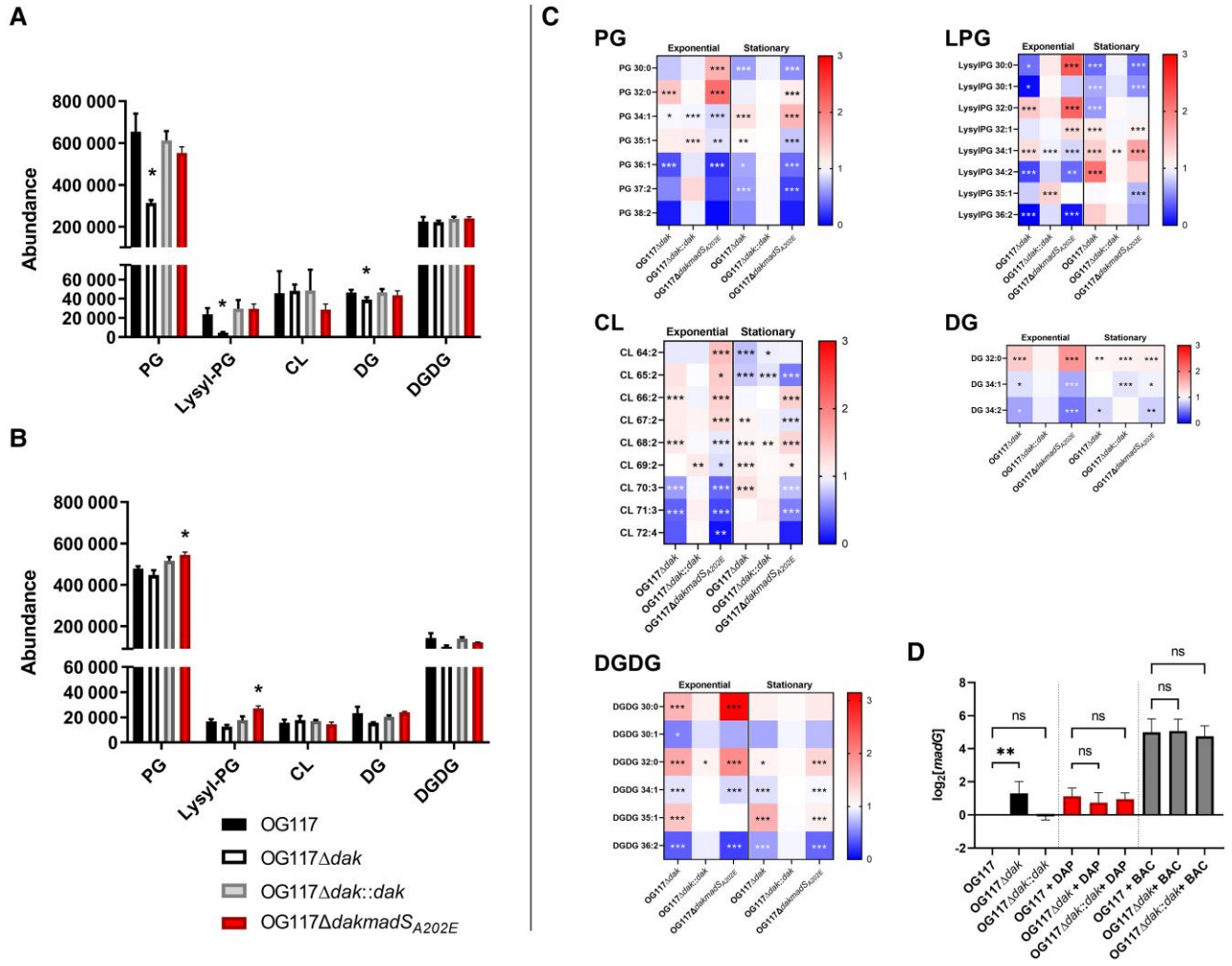

Figure 3. Deletion of *dak* is associated with changes in membrane fatty acyl composition and alteration of *madG* expression. Lipid analysis was carried out using hydrophilic interaction chromatography-ion mobility-mass spectrometry. Total lipids in (*A*) exponential growth and (*B*) stationary phase were determined in the OG117 and *dak* deletion strains. Relative abundance is on the y-axis, and each major enterococcal lipid species is on the x-axis. Significant differences in abundance of PG, lysyl-PG, and DG were seen in the *dak* deletion strain at exponential phase, but not stationary phase. The OG117Δ*dakmadS*$_{A202E}$ strain developed a spontaneous mutation that led to derepression of the *fab* operon (see text). No differences were observed in this strain in exponential phase, but there was a significant increase in PG and lysyl-PG at stationary phase. *C*, Fatty acyl chain composition of PG, LPG, CL, DG, and DGDG in exponential and stationary phase are shown as a heat map based on relative change from wild-type OG117, with red representing an increase and blue representing a decrease in the relative proportion of each species. Carbon chain length and number of unsaturated bonds are given (eg, PG 34:1). Both strains with the *dak* deletion showed a similar acyl chain profile, despite the constitutive activation of the FASII system in the OG117Δ*dakmadS*$_{A202E}$ mutant. *D*, Expression of *madG* at exponential phase in the *dak* deletion strains using qRT-PCR, without antibiotics (black bars), with DAP (red bars), and with BAC (grey bars). In the absence of antibiotic stress, there was a significant 2.5-fold increase in *madG* expression in the OG117Δ*dak* strain as compared to OG117. Under daptomycin and bacitracin stress, there was no significant difference in *madG* expression between the strains. Error bars represent the standard deviation from three independent runs. **P* < .05, ***P* < .01, ****P* < .001. Abbreviations: BAC, bacitracin; CL, cardiolipin; DAP, daptomycin; DG, diacylglycerol; DGDG, digalactosyldiacylglycerol; LPG, lysyl-PG; ns, not significant; PG, phosphatidylglycerol; qRT-PCR, quantitative reverse-transcription polymerase chain reaction.

with and without antibiotic stress in the *dak* mutant strains during exponential growth (Figure 3*D*). In the absence of antibiotic stress, there was a 2-fold increase in the expression of *madG* in the *dak* deletion mutant as compared to OG1RF, similar to the 2-fold induction of *madG* expression seen after exposure to daptomycin in all strains. Bacitracin led to a robust expression of *madG* that did not differ across strains. Taken together, our results suggest that changes in phospholipid composition due to the deletion of *dak* both directly contribute to CAMP resistance and prime the transcriptional response of the MadRS system.

MadRS Is Associated With CAMP-Dependent Changes in Survival of *Caenorhabditis elegans*

Using a *C. elegans* infection model, we examined the role of the MadRS system in protecting enterococci from CAMPs produced by the innate immune system. In wild-type *C. elegans*, there was an attenuation of the OG1RFΔ*madR* strain as compared to OG1RF and OG1RF*madS*$_{A202E}$ (Figure 4*A* and 4*B*). This phenotype was reversed with complementation of *madR* on a plasmid with minimal differences between OG1RF and the complemented strain. Next we performed the same survival

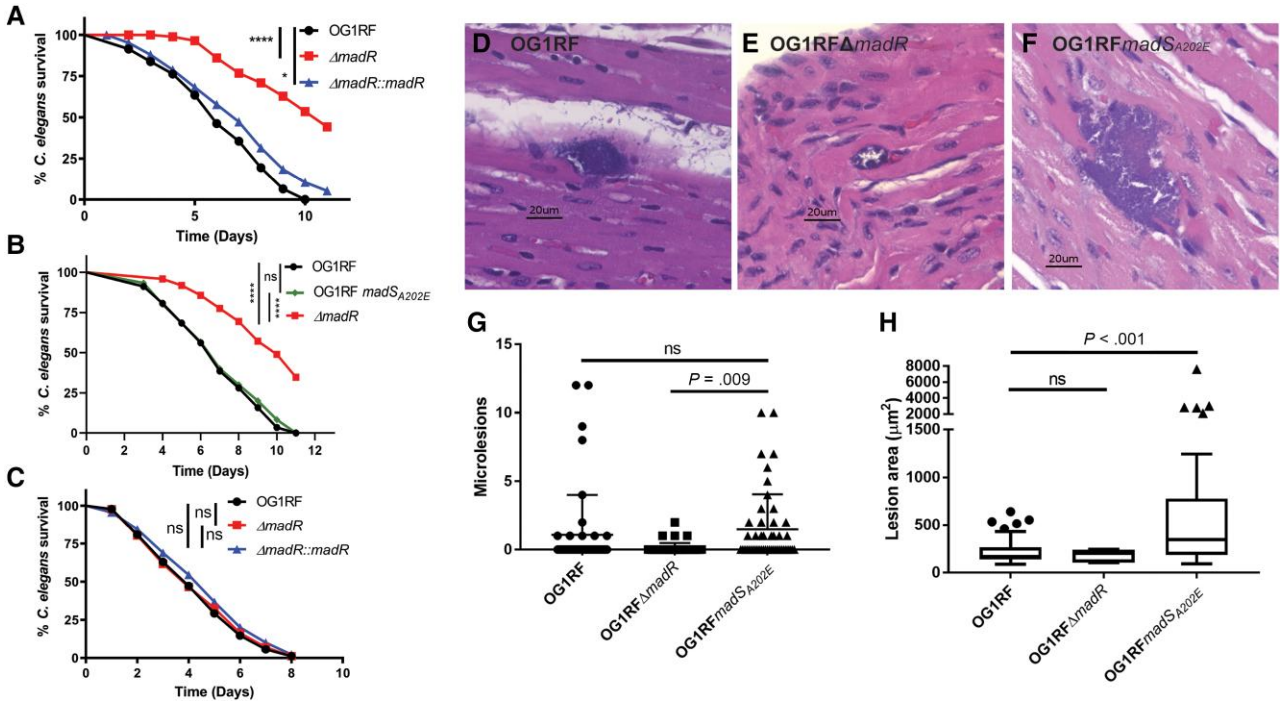

Figure 4. The MadRS system protects *Enterococcus faecalis* from the host immune response in vivo. Nematode survival in a *Caenorhabditis elegans* model of infection with (*A* and *B*) wild-type nematodes and (*C*) *pmk-1* knockouts deficient in antimicrobial peptide production. Nematodes showed increased survival when infected with the OG1RFΔ*madR* strain as compared to the wild-type OG1RF, OG1RF*madS*$_{A202E}$, or when *madR* was complemented in *trans* on a plasmid; however, no differences in survival were seen in the nematodes unable to produce antimicrobial peptides. Infection with the OG1RF*madS*$_{A202E}$ strain was associated with similar nematode survival as wild-type OG1RF, suggesting that activation of MadRS does not increase virulence. *D–F*, Cardiac microlesions were assessed in a mouse model of peritonitis for the OG1RF, OG1RFΔ*madR*, and OG1RF*madS*$_{A202E}$ strains. Murine hearts were formalin fixed and embedded in paraffin, bisected, then sectioned on a microtome. Representative micrographs of hematoxylin and eosin stained sections are shown. *G*, Average number of cardiac microlesions per section. Eight sections were evaluated per animal and 48 in total for each strain. Differences in the mean number of microlesions between each strain were determined using 1-way ANOVA. *P* values are indicated for each comparison on the graph. *H*, Lesion area in μm^2 are given as box and whisker plots of inner quartile range, with error bars plotted by the method of Tukey. Outliers are shown as individual data points. Statistical differences between strains were assessed using the Kruskal-Wallis test. *P* values are indicated for each comparison on the graph. $^*P < .05$, $^{****}P < .0001$; ns, not significant.

assay in *C. elegans* lacking the *pmk-1* gene, which encodes an ortholog of the p38 MAP kinase necessary for production of CAMPs. Figure 4*C* shows that there were no differences in survival between Δ*pmk-1* worms infected with OG1RF, OG1RFΔ*madR*, or the complemented strain, supporting the notion that the presence of CAMPs mediates survival of *C. elegans* infected with *E. faecalis* lacking MadR, rather than a change in strain virulence.

The *madS*$_{A202E}$ Allele Is Associated With an Increased Burden of Cardiac Microlesions in a Mouse Peritonitis Model of Infection

Given the importance of host CAMPs to the innate immune response, we sought to investigate the in vivo impact of the MadRS system in a mouse model of peritonitis. We examined overall survival, bacterial burden in the spleen, and the average number and size of cardiac microlesions as assessed by histopathology of cardiac tissue from infected mice [29]. There was no difference in median survival or bacterial burden in the spleen between OG1RF, OG1RFΔ*madR*, and OG1RF*madS*$_{A202E}$ (Supplementary Figure 4). However, mice infected with OG1RF*madS*$_{A202E}$ showed an increase in the mean number of cardiac microlesions per histopathological section as compared to OG1RFΔ*madR* (Figure 4*D–H*), and a significantly larger lesion area as compared to OG1RF.

DISCUSSION

The potential for cross-resistance between antibiotics and CAMPs of the innate immune system is of particular concern. Vancomycin resistant enterococcal (VRE) colonization of the gastrointestinal (GI) tract has been demonstrated to be a precursor to mucosal translocation and bloodstream infections, particularly in the immunocompromised host [34–36]. In this setting, enterococcal exposure to CAMPs in the GI tract can prime antibiotic resistance and may have implications for the use of daptomycin in treating VRE infections, especially as monotherapy. This study characterizes a defense network that protects the enterococcal cell envelope from CAMPs and peptide-like antibiotics.

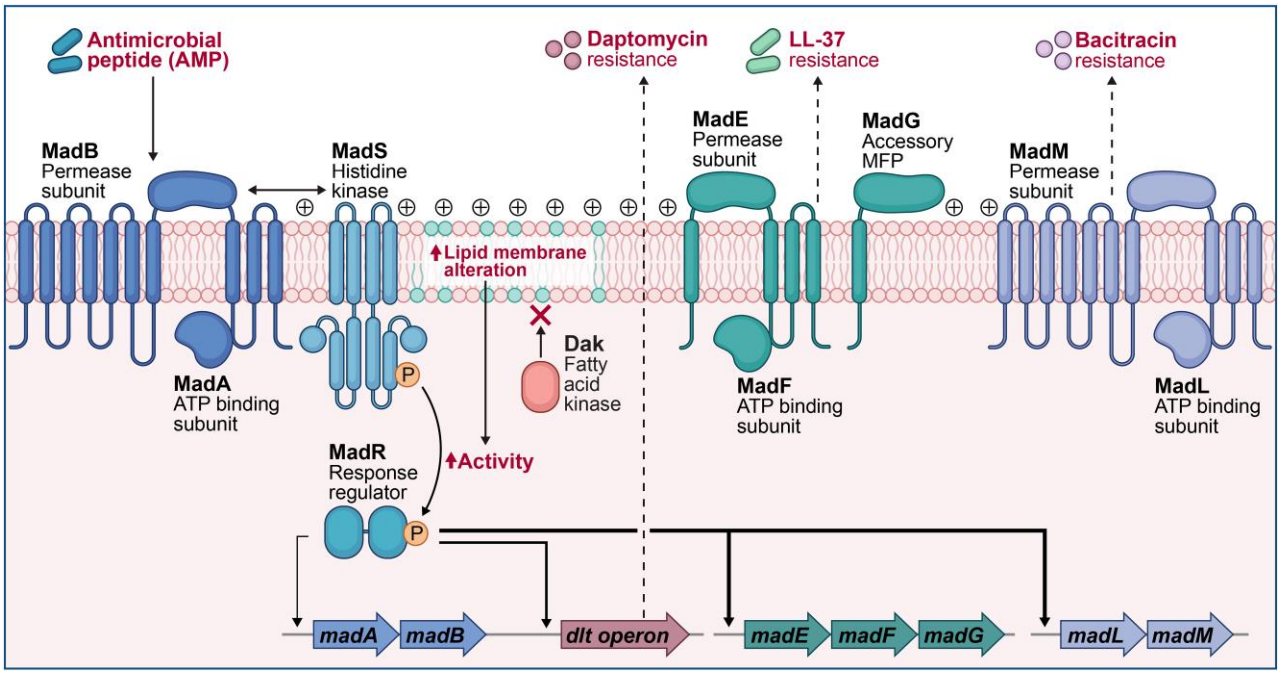

Figure 5. Model for the function of the membrane antimicrobial peptide defense system. The MadRS system controls a network of effector proteins that provide a coordinated and specific defense against cationic antimicrobial peptides (CAMPs) and CAMP-like antibiotics. The MadS sensor histidine kinase is activated by the flux-sensing mechanism of the constitutively expressed MadAB ATP-binding cassette (ABC) transporter in the presence of AMPs. This leads to phosphorylation of the MadR response regulator and upregulation of the genes encoding MadEFG, MadLM, and the *dlt* operon, as well as *mprF2* and the gene encoding a putative peptidoglycan hydrolase SalA (not pictured). The width of the arrows approximates the strength of association for each interaction. These targets each provide protection from their specific substrates including bacitracin (MadLM), LL-37 and HBD3 (MadEFG), and daptomycin (DltABCD). After removal of CAMPs from the membrane by the ABC transporters, D-alanylation of teichoic acids and lysylation of phosphotidylglycerol alters cell surface charge and prevents diffusion of these molecules back to the cell membrane surface. Loss of Dak function leads to alterations of the cell membrane lipids, which primes expression of the MadRS system and may also directly interfere with CAMP binding.

Our transcriptional analysis shows that the MadRS system has a much broader cell envelope protective effect than previously known (Figure 5). Consistent with prior results, MadR controls expression of MadLM and also results in an increase in the expression of the *dlt* operon [37]. In addition, MadR appears to regulate the expression of the peptidoglycan hydrolase SalA, the lysylphosphatidylglycerol synthetase MprF2, and the novel *madEFG* operon. The *madEFG* genes share sequence identity with the *spr0693-0695* operon in *Streptococcus pneumoniae*, which encode a MacAB-like efflux pump with LL-37 as a potential substrate [38]. The product of *spr0693* was predicted to form a hexameric channel of approximately 155 Å, potentially spanning the peptidoglycan layer. We postulate that MadEFG is likely to function by removing CAMPs from the membrane interface and transporting them past the peptidoglycan layer. Concomitantly, the MadRS regulon alters the cell envelope by D-alanylation of wall teichoic acids via Dlt or production of lysylphosphatidylglycerol via MprF to prevent diffusion of CAMPs back to the membrane surface. Interestingly, no obvious homologues of *madEFG* are present in the genome of *Enterococcus faecium* DO, suggesting that there are important differences in the mechanism underlying membrane defense between *E. faecalis* and *E. faecium*.

Alterations of the membrane bilayer, observed in the *dak* knockout, may provide a further barrier to effective CAMP action. Loss of Dak function resulted in a membrane lipid fatty acid profile that contained significantly more saturated fatty acids, in part explaining our prior observation of decreased membrane fluidity in the Dak mutant [5]. These changes were sufficient to decrease the activity of HBD3, and also appear to prime the MadRS system by leading to an increase in the baseline transcription of target genes. Thus, the membrane lipid environment has both a direct and indirect role in antimicrobial resistance. These findings may explain why mutations in both phospholipid metabolism and cell envelope stress response networks emerge together in daptomycin-resistant isolates.

The MadRS response appears to complement the global stress response of LiaFSR. Recently, a link between the LiaFSR and MadRS systems was demonstrated in *E. faecalis*, with activation of the LiaFSR system associated with increased expression of MadRS [39]. MadAB-MadS are likely to function via a flux-sensing mechanism, where the transport activity of MadAB is coupled to the kinase activity of MadS [40]. The data presented here suggest that the emergence of daptomycin resistance via MadRS arises via a decoupling of the MadS kinase and the MadAB flux sensor, as the $MadS_{A202E}$ mutant showed

increased expression of the genes of the MadR regulon, even in the absence of antibiotic stress. This decoupling bypassed the potential transcriptional regulation of the MadRS system by LiaFSR, and activation of MadRS results in a survival advantage against CAMPs, even in the absence of *liaR*.

The results from the *C. elegans* and mouse peritonitis models suggest that the MadRS system also plays a major role against CAMPs in vivo, and resistance arising via this pathway may have implications for the clearance of deep-seated infections such as infective endocarditis. Interestingly, we did not see a difference in bacterial burden in the spleen. One possibility is that immune-mediated clearance via macrophages and neutrophils may be preserved via activity of alternate peptides such as HNP-1, the activity of which was not affected in our assay conditions. Because peptides such as β-defensins and cathelicidins are an important part of mucosal barrier defense, this resistance pattern may predispose to invasive infection and bacteremia, particularly in immunocompromised hosts with neutropenia [41, 42]. These studies were performed with a laboratory enterococcal strain, and further work is needed to understand the role of this system in clinical isolates with respect to colonization of the GI tract and subsequent risk for translocation and infection.

Supplementary Data

Supplementary materials are available at *The Journal of Infectious Diseases* online (http://jid.oxfordjournals.org/). Supplementary materials consist of data provided by the author that are published to benefit the reader. The posted materials are not copyedited. The contents of all supplementary data are the sole responsibility of the authors. Questions or messages regarding errors should be addressed to the author.

Notes

Acknowledgments. The authors thank Rafael Rios for assistance with the RNA sequence analysis and Rachael Whitehead for graphical design.

Data availability. Datasets for the whole-genome sequencing and RNA sequences are available at the National Center for Biotechnology Information (NCBI) under Bioproject Accession number PRJNA1025297.

Financial support. This work was supported by National Institute of Health, National Institute of Allergy and Infectious Diseases (NIH/NIAID) (grant number K08 AI135093 to W. R. M.); NIH/NIAID (grant numbers K24 AI121296, R01 AI148342, R01 AI134637, and P01 AI152999 to C. A. A.); NIH (grant numbers R01 DE027608, R01 AI150045, and R21 AI167124 to D. A. G.); NIH/NIAID training fellowship from the Gulf Coast Consortia, Texas Medical Center Training Program in Antimicrobial Resistance (grant number T32 AI141349 to S. L. E.); NIH/NIAID (grant number R01 A1080714 to Y. S.); and NIH/NIAID (grant number R01 AI136979 to L. X.).

Potential conflicts of interest. W. R. M. has received grant support from Merck; and royalties from UpToDate. C. A. A. has received royalties from UpToDate. All other authors report no potential conflicts.

All authors have submitted the ICMJE Form for Disclosure of Potential Conflicts of Interest. Conflicts that the editors consider relevant to the content of the manuscript have been disclosed.

References

1. Weiner-Lastinger LM, Abner S, Edwards JR, et al. Antimicrobial-resistant pathogens associated with adult healthcare-associated infections: summary of data reported to the National Healthcare Safety Network, 2015–2017. Infect Control Hosp Epidemiol **2020**; 41:1–18.
2. Miller WR, Murray BE, Rice LB, Arias CA. Resistance in vancomycin-resistant enterococci. Infect Dis Clin North Am **2020**; 34:751–71.
3. Dubin K, Pamer EG. Enterococci and their interactions with the intestinal microbiome. Microbiol Spectr **2014**; 5: 10.1128/microbiolspec.BAD-0014-2016.
4. Arias CA, Panesso D, McGrath DM, et al. Genetic basis for in vivo daptomycin resistance in enterococci. N Engl J Med **2011**; 365:892–900.
5. Miller WR, Tran TT, Diaz L, et al. LiaR-independent pathways to daptomycin resistance in *Enterococcus faecalis* reveal a multilayer defense against cell envelope antibiotics. Mol Microbiol **2019**; 111:811–24.
6. Prater AG, Mehta HH, Kosgei AJ, et al. Environment shapes the accessible daptomycin resistance mechanisms in *Enterococcus faecium*. Antimicrob Agents Chemother **2019**; 63:e00790-19.
7. Tran TT, Panesso D, Gao H, et al. Whole-genome analysis of a daptomycin-susceptible *Enterococcus faecium* strain and its daptomycin-resistant variant arising during therapy. Antimicrob Agents Chemother **2013**; 57:261–8.
8. Miller WR, Bayer AS, Arias CA. Mechanism of action and resistance to daptomycin in *Staphylococcus aureus* and enterococci. Cold Spring Harb Perspect Med **2016**; 6:a026997.
9. Khan A, Davlieva M, Panesso D, et al. Antimicrobial sensing coupled with cell membrane remodeling mediates antibiotic resistance and virulence in *Enterococcus faecalis*. Proc Natl Acad Sci U S A **2019**; 116:26925–32.
10. Prater AG, Mehta HH, Beabout K, et al. Daptomycin resistance in *Enterococcus faecium* can be delayed by disruption of the LiaFSR stress response pathway. Antimicrob Agents Chemother **2021**; 65:e01317-20.
11. Dintner S, Staron A, Berchtold E, Petri T, Mascher T, Gebhard S. Coevolution of ABC transporters and two-component regulatory systems as resistance modules against antimicrobial peptides in Firmicutes bacteria. J Bacteriol **2011**; 193:3851–62.

12. Parsons JB, Broussard TC, Bose JL, et al. Identification of a two-component fatty acid kinase responsible for host fatty acid incorporation by *Staphylococcus aureus*. Proc Natl Acad Sci U S A **2014**; 111:10532–7.
13. Harp JR, Saito HE, Bourdon AK, et al. Exogenous fatty acids protect *Enterococcus faecalis* from daptomycin-induced membrane stress independently of the response regulator LiaR. Appl Environ Microbiol **2016**; 82:4410–20.
14. Debroy S, van der Hoeven R, Singh KV, et al. Development of a genomic site for gene integration and expression in *Enterococcus faecalis*. J Microbiol Methods **2012**; 90:1–8.
15. Price VJ, Huo W, Sharifi A, Palmer KL. CRISPR-Cas and restriction-modification act additively against conjugative antibiotic resistance plasmid transfer in *Enterococcus faecalis*. mSphere **2016**; 1:e00064-16.
16. Reyes J, Panesso D, Tran TT, et al. A liaR deletion restores susceptibility to daptomycin and antimicrobial peptides in multidrug-resistant *Enterococcus faecalis*. J Infect Dis **2015**; 211:1317–25.
17. Jones T, Yeaman MR, Sakoulas G, et al. Failures in clinical treatment of *Staphylococcus aureus* infection with daptomycin are associated with alterations in surface charge, membrane phospholipid asymmetry, and drug binding. Antimicrob Agents Chemother **2008**; 52:269–78.
18. Garrett TA, Guan Z, Raetz CRH. Analysis of ubiquinones, dolichols, and dolichol diphosphate-oligosaccharides by liquid chromatography-electrospray ionization-mass spectrometry. Methods Enzymol **2007**; 432:117–43.
19. Garrett TA, Kordestani R, Raetz CRH. Quantification of cardiolipin by liquid chromatography-electrospray ionization mass spectrometry. Methods Enzymol **2007**; 433: 213–30.
20. Bligh EG, Dyer WJ. A rapid method of total lipid extraction and purification. Can J Biochem Physiol **1959**; 37:911–7.
21. Hines K, Herron J, Xu L. Assessment of altered lipid homeostasis by HILIC-ion mobility-mass spectrometry-based lipidomics. J Lipid Res **2017**; 58:809–19.
22. Hines KM, Waalkes A, Penewit K, et al. Characterization of the mechanisms of daptomycin resistance among gram-positive bacterial pathogens by multidimensional lipidomics. mSphere **2017**; 2:e00492-17.
23. Hines KM, May JC, McLean JA, Xu L. Evaluation of collision cross section calibrants for structural analysis of lipids by traveling wave ion mobility-mass spectrometry. Anal Chem **2016**; 88:7329–36.
24. Ulmer CZ, Koelmel JP, Ragland JM, Garrett TJ, Bowden JA. LipidPioneer: a comprehensive user-generated exact mass template for lipidomics. J Am Soc Mass Spectrom **2017**; 28:562–5.
25. Ross DH, Cho JH, Zhang R, Hines KM, Xu L. Lipydomics: a python package for comprehensive prediction of lipid collision cross sections and retention times and analysis of ion mobility-mass spectrometry-based lipidomics data. Anal Chem **2020**; 92:14967–75.
26. Garsin DA, Sifri CD, Mylonakis E, et al. A simple model host for identifying gram-positive virulence factors. Proc Natl Acad Sci U S A **2001**; 98:10892–7.
27. Kim DH, Feinbaum R, Alloing G, et al. A conserved p38 MAP kinase pathway in *Caenorhabditis elegans* innate immunity. Science **2002**; 297:623–6.
28. Singh KV, Arias CA, Murray BE. Efficacy of tedizolid against enterococci and staphylococci, including cfr^+ strains, in a mouse peritonitis model. Antimicrob Agents Chemother **2019**; 63:e02627-18.
29. Brown AO, Singh KV, Cruz MR, et al. Cardiac microlesions form during severe bacteremic *Enterococcus faecalis* infection. J Infect Dis **2021**; 223:508–16.
30. Schindelin J, Arganda-Carreras I, Frise E, et al. Fiji: an open-source platform for biological-image analysis. Nat Methods **2012**; 9:676–82.
31. Popella P, Krauss S, Ebner P, Nega M, Deibert J, Götz F. Vrah is the third component of the *Staphylococcus aureus* VraDEH system involved in gallidermin and daptomycin resistance and pathogenicity. Antimicrob Agents Chemother **2016**; 60:2391–401.
32. Gebhard S, Fang C, Shaaly A, et al. Identification and characterization of a bacitracin resistance network in *Enterococcus faecalis*. Antimicrob Agents Chemother **2014**; 58:1425–33.
33. Zuo G, Chen ZP, Jiang YL, et al. Structural insights into repression of the pneumococcal fatty acid synthesis pathway by repressor FabT and co-repressor acyl-ACP. FEBS Lett **2019**; 593:2730–41.
34. DiPippo AJ, Tverdek FP, Tarrand JJ, et al. Daptomycin non-susceptible *Enterococcus faecium* in leukemia patients: role of prior daptomycin exposure. J Infect **2017**; 74:243–7.
35. Ubeda C, Taur Y, Jenq RR, et al. Vancomycin-resistant *Enterococcus* domination of intestinal microbiota is enabled by antibiotic treatment in mice and precedes bloodstream invasion in humans. J Clin Invest **2010**; 120:4332–41.
36. Ramos Y, Sansone S, Hwang SM, et al. Remodeling of the enterococcal cell envelope during surface penetration promotes intrinsic resistance to stress. mBio **2022**; 13: e0229422.
37. Diagne AM, Pelletier A, Durmort C, et al. Identification of a two-component regulatory system involved in antimicrobial peptide resistance in *Streptococcus pneumoniae*. PLoS Pathog **2022**; 18:e1010458.
38. Yang HB, Hou WT, Cheng MT, Jiang YL, Chen Y, Zhou CZ. Structure of a MacAB-like efflux pump from *Streptococcus pneumoniae*. Nat Commun **2018**; 9:196.
39. Morris SM, Fritz G, Rogers T, Gebhard S. Novel regulatory logic in the antibiotic resistance response of *Enterococcus faecalis* against cell envelope targeting antibiotics. BioRxiv,

doi: 10.1101/2022.11.16.516778, 16 November **2022**, preprint: not peer reviewed.
40. George NL, Orlando BJ. Architecture of a complete Bce-type antimicrobial peptide resistance module. Nat Commun **2023**; 14:3896.
41. Ganz T. Defensins: antimicrobial peptides of innate immunity. Nat Rev Immunol **2003**; 3:710–20.
42. Hooper LV, Macpherson AJ. Immune adaptations that maintain homeostasis with the intestinal microbiota. Nat Rev Immunol **2010**; 10:159–69.